Applied Physics Letters

RESEARCH ARTICLE | AUGUST 05 2024

Waveguide-based microscope slide for label-free high-resolution imaging FREE

Songlin Yang ; Qihao Sun; Yurong Cao ; Yong-Hong Ye ; Jiayu Zhang

Check for updates

Appl. Phys. Lett. 125, 063701 (2024)
https://doi.org/10.1063/5.0225792

View Online
Export Citation

07 August 2024 01:21:30

Nanotechnology & Materials Science
Optics & Photonics
Impedance Analysis
Scanning Probe Microscopy
Sensors
Failure Analysis & Semiconductors



Unlock the Full Spectrum.
From DC to 8.5 GHz.
Your Application. Measured.
Find out more
Zurich Instruments

AIP Publishing

Applied Physics Letters ARTICLE pubs.aip.org/aip/apl

Waveguide-based microscope slide for label-free high-resolution imaging

Cite as: Appl. Phys. Lett. **125**, 063701 (2024); doi: 10.1063/5.0225792
Submitted: 27 June 2024 · Accepted: 25 July 2024 ·
Published Online: 5 August 2024

View Online Export Citation CrossMark

Songlin Yang,[1,a)] Qihao Sun,[2] Yurong Cao,[1] Yong-Hong Ye,[1] and Jiayu Zhang[2]

AFFILIATIONS

[1]School of Computer and Electronic Information, Nanjing Normal University, Nanjing 210023, China
[2]School of Electronic Science and Engineering, Southeast University, Nanjing 210096, China

[a)]Author to whom correspondence should be addressed: slyang@njnu.edu.cn

ABSTRACT

Waveguide-based total internal reflection fluorescence microscopy has been widely adopted due to its excellent signal-to-noise ratio over a large field of view. However, with the increasing demand for label-free imaging, waveguide-based evanescent light scattering microscopy (ESM) has also garnered significant attention. Here, we present a low-cost waveguide-based microscope slide that offers easier integration with conventional optical microscopy. This microscope slide uses an incoherent light source coupled to a lithium tantalate (LT) planar waveguide to generate an evanescent light that illuminates samples located within a few hundred nanometers of the waveguide surface. We perform its application for imaging chromium nanoholes and polystyrene nanospheres, demonstrating its label-free, high-resolution, high-contrast imaging performance. LT waveguide microscope slides provide a simple and effective solution for ESM.

Published under an exclusive license by AIP Publishing. https://doi.org/10.1063/5.0225792

07 August 2024 01:21:30

The visualization of nanoscale objects provides valuable insight into the fundamental properties of matter. Detecting the scattered light emitted by nanoscale objects is key to their microscopic imaging. However, when the dimensions of objects are significantly smaller than the wavelength of the illumination, the limited interaction between the light and the object makes it challenging to detect the scattered light. To overcome this challenge, it is necessary to enhance the specificity of the scattered signal or improve the sensitivity of the imaging system through techniques such as fluorescence labeling[1,2] and surface plasmon resonance.[3,4]

In addition to focusing on the scattered signals emitted by objects, one should not ignore the background signals generated by the illumination, substrate, and surrounding objects, which are the main source of degradation of the signal of interest. With conventional bright-field illumination, the largest contribution of background signals arises from the illumination field, which makes it very difficult to detect the weak signal from a nanoscale object. Dark-field imaging techniques improve the signal-to-noise ratio (SNR) of valuable signals by suppressing background light. However, the large depth of field of the objective lens causes the imaging system to collect out-of-focus light that blurs valuable signals. Total internal reflection fluorescence microscopy (TIRFM) uses evanescent waves to selectively excite fluorescent molecules with dimensions smaller than 100 nm. This excitation effectively attenuates out-of-focus fluorescence, enabling high SNR imaging of individual molecules on the surface.[5–7]

In recent years, there has been a surge in interest among researchers in waveguide-based TIRFM.[8] It can achieve imaging with large field-of-view (FOV) reaching up to millimeter scales[9,10] and support super-resolution techniques, including direct stochastic optical reconstruction microscopy (dSTORM)[11] and structured light illumination microscopy (SIM).[12] Meanwhile, it is evident that waveguide-based label-free imaging will emerge as a prominent technology, especially considering the limitations of fluorescent labeling and its potential for broader applications. A recent study has demonstrated the label-free imaging of single proteins by objective lens-based evanescent light scattering microscopy (ESM).[13] The detection of faint objects using waveguide-based ESM without the need for labeling has also been demonstrated.[14–16] The coherent speckle noise can be reduced when using a multimode waveguide as a partially coherent illumination.[17] Compared to conventional dark-field imaging, waveguide-based ESM provides an excellent SNR with minimal background signals.[18] Although waveguide-based TIRFM and ESM have been extensively studied, there is still potential for further simplification. The use of microscope slides as waveguides represents a simplified design that has been successfully demonstrated,[19] Microscope slides with higher refractive indices will provide larger transverse modes for evanescent light illumination, which can effectively reduce background signals and enhance the imaging system's ability to detect high-frequency signals.

Published under an exclusive license by AIP Publishing

In this Letter, we introduce a simple and innovative microscope slide that exhibits exceptional imaging contrast, inspired by ESM. This microscope slide uses an incoherent optical fiber end-fire coupled to a lithium tantalate (LT) planar waveguide to generate an evanescent light that illuminates samples located within a few hundred nanometers of the waveguide surface. We refer to it as ESM based on LT microscope slide (LTms). We first demonstrate high-resolution and high-contrast imaging of metal and transparent objects such as chromium (Cr) nanoholes and polystyrene (PS) nanospheres. The working mechanism of the ESM-LTms is then analyzed by simulating the electric field distribution. The simulation results show that the sample interacts with the evanescent waves distributed on the surface of LTms, and some of the evanescent waves escape from the near field and scatter into the far field. Finally, the effect of the propagation direction and transverse wave vector of the evanescent waves on the resolution of ESM-LTms is investigated by simulation. Considering the simplicity of the ESM-LTms, this method will be easier to integrate and generalize with conventional optical microscopy.

The ESM-LTms described here is shown in Fig. 1, which consists of an upright optical microscope (Leica DM2500 M), a square LT plate (length: 20 mm, thickness: 1 mm, purchased from Jiaozuo King's Photonics Co., Ltd), and an optical fiber-coupled part. The monochromatic LED light with a central wavelength of 500 nm is coupled to the LT plate through the end-fire of the optical fiber with a diameter of 800 μ m. Due to total reflection, the light coupled to the LT plate forms an evanescent field distribution on the surface of the LT plate. Here, the sides of the LTms are not polished for use as a scattering layer. It is used to widen the incidence angle of light coupled to the LT plate in order to increase the amount of total reflected light. LT plates are uniaxial crystals that exhibit birefringence for incident light, where the ordinary and extraordinary refractive indices are $n_o = 2.176$ and $n_e = 2.180$, respectively. Because LTms has a higher refractive index than conventional glass slides ($n = 1.46 - 1.78$), higher transverse modes of evanescent light will appear in the multimode evanescent light illumination produced by LTms, which is beneficial for imaging systems to detect high spatial frequency information. The orientation of the optical axis in the LTms is not specially selected, and the birefringent effect causes stray light to be transmitted from the side and top surfaces at the edge positions of the LTms, thereby blurring object signals. To minimize the effect of stray light on imaging, a layer of light-blocking patches with a central opening, serving as a working window (length: 6 mm), is applied to cover the upper surface of LTms. The scattered signals generated by the interaction between the sample and the evanescent wave within the working window are collected by the objective lens with a numerical aperture (NA) of 0.9 and finally imaged into the sCMOS camera (Teledyne Photometrics Prime BSI, pixel size 6.5 μm, 4.2 megapixel).

First, to demonstrate the imaging capability of the ESM-LTms, we fabricated the paired Cr nanoholes with a diameter of 200 nm on top of the LTms through a series of nanofabrication processes including Cr film deposition (thickness: 50 nm), electron beam lithography (EBL), and etching. Figures 2(a) and 2(b) depict the images of the Cr nanoholes obtained by conventional optical microscopy and ESM-LTms, respectively. It can be observed from Fig. 2 that the image obtained by ESM-LTms has high resolution and contrast. In order to quantitatively analyze the imaging results, the cross section intensity distributions extracted from the images of the Cr nanohole pairs are plotted in Figs. 2(c) and 2(d). According to Rayleigh's criterion, Cr nanoholes with edge-to-edge distances of 200 and 250 nm cannot be resolved by conventional optical microscopy, but can be resolved by ESM-LTms. Figure 2 reveals that ESM-LTms provides higher resolution compared to conventional optical microscopy.

The strength of the interaction between light and an object should be related to the polarizability of the object, which is a measure of its ability to respond and interact with incident electromagnetic waves.[20] Nanoscale objects much smaller than the diffraction limit can usually be approximated as dipoles, with polarizabilities given by $\alpha = 3\varepsilon_m V\left(\frac{\varepsilon_p - \varepsilon_m}{\varepsilon_p + 2\varepsilon_m}\right)$, where ε_m and ε_p are the complex permittivity of the medium and particle, respectively, and V is its volume.[21] The scattering cross section determines the signal strength of a non-resonant nanoscale object, which can be expressed as $\sigma_{scat} = \frac{8}{3\pi^2}|\alpha|^2\lambda^{-4}$, for spherical nanoscale objects, a reduction in the diameter of a sphere by

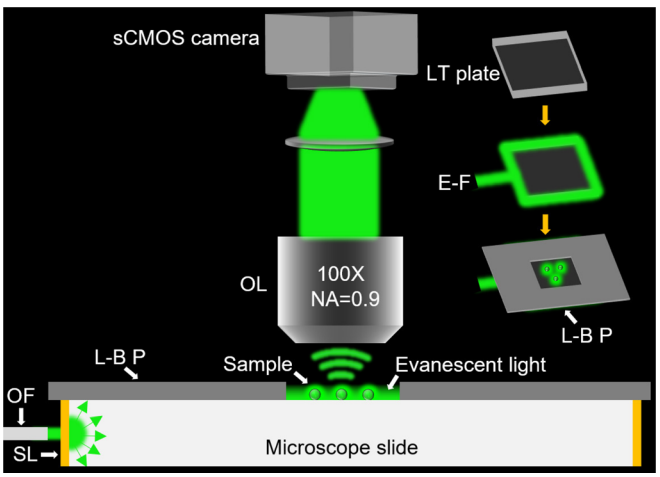


FIG. 1. Schematic of the ESM-LTms system. OL: objective lens; L-B P: light-blocking patches; OF: optical fiber; SL: scattering layer; E-F: end-fire.

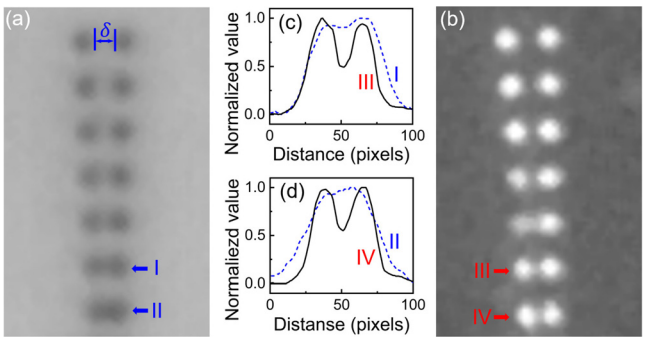


FIG. 2. Demonstration of ESM-LTms imaging performance by imaging 200 nm diameter Cr nanoholes. The edge-to-edge distance δ of Cr nanohole pairs ranges from 200 to 500 nm, with increments of 50 nm. (a) The conventional diffraction-limited images. (b) The ESM-LTms images. (c)–(d) The corresponding intensity cross section comparison. The dashed lines and solid lines correspond to the intensity cross section of the conventional diffraction-limited images and the ESM-LTms images, respectively.

07 August 2024 01:21:30

Published under an exclusive license by AIP Publishing

a factor of 10 reduces the intensity of scattered light by 10^6 for a given incident photon flux.[20] This is the main reason why label-free objects are difficult to detect when their dimensions are much smaller than the diffraction limit. The permittivity of a transparent object only represents its real part, while the absorption of incident light is negligible. Therefore, detecting phase changes becomes the preferred contrast mechanism for imaging transparent objects. When phase changes are not taken into consideration, the extremely weak scattered signals of transparent objects make high-resolution imaging challenging. We next investigated the ability of ESM-LTms to visualize weakly scattering samples by imaging label-free PS nanospheres with a diameter of 100 nm. The images of PS nanospheres obtained by conventional optical microscopy and ESM-LTms are presented in Figs. 3(a) and 3(b), respectively. The cross section intensity distributions of adjacent PS nanospheres with representation are illustrated in Figs. 3(c) and 3(d). Figure 3 reveals that ESM-LTms also has high contrast when imaging transparent PS nanospheres.

To investigate the imaging mechanism of ESM-LTms, we simulated the electric field intensity distribution of Cr nanoholes and PS nanospheres on the upper surface of the waveguide under single-mode evanescent light illumination by the finite-difference time-domain (FDTD) method. The longitudinal cross section of the model for this simulation is shown in Fig. 4(a), where we used a three-dimensional model in which all boundaries are perfectly matched layers (PML), a mode light source is used to generate waveguide-based evanescent light illumination, and the mesh accuracy is 4 nm. The surface of the waveguide distributes evanescent light with a transverse wave vector of $2\,k_0$ and its phase distribution is shown in Fig. 4(b). Figures 4(c) and 4(d) show the electric field intensity distributions around the Cr nanoholes and PS nanospheres on the waveguide, respectively. Figure 4(c) shows the leakage of light from the top of the Cr nanohole, which may be

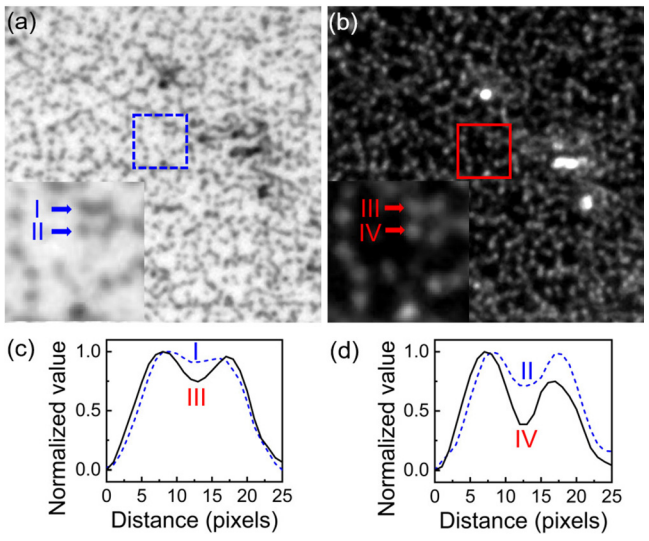


FIG. 3. Demonstration of ESM-LTms imaging performance by imaging 100 nm diameter PS nanospheres. (a) The conventional diffraction-limited images. (b) The ESM-LTms images. (c) and (d) The corresponding intensity cross section comparison. The dashed lines and solid lines correspond to the intensity cross section of the conventional diffraction-limited images and The ESM-LTms images, respectively.

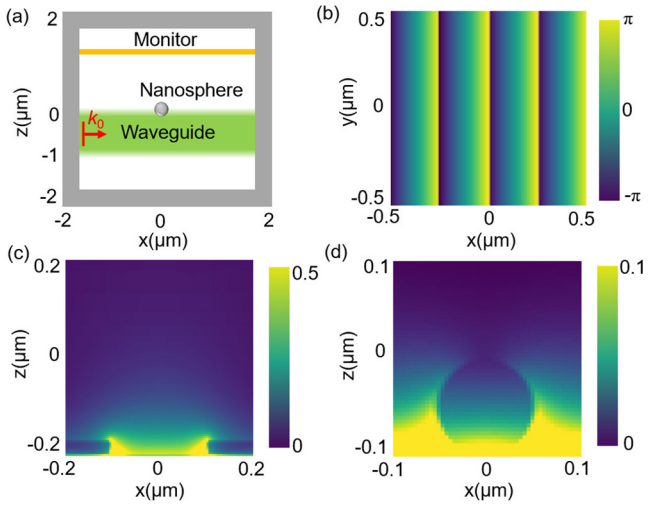


FIG. 4. Demonstration of the ESM-LTms imaging mechanisms. (a) Schematic of the simulation model. (b) Phase distribution of the evanescent wave with a transverse wave vector of $2\,k_0$. (c) and (d) Longitudinal cross section electric field intensity distributions corresponding to Cr nanoholes and PS nanospheres located within the evanescent wave with a transverse wave vector of $2\,k_0$, respectively.

formed by the conversion of evanescent waves into propagating waves. Light at the entrance of a narrow slit produces evanescent waves with high transverse wave vectors k_x or k_y.[22] Due to the convolution of these high transverse modes with the exit aperture, a significant portion of the transverse modes acquire values of k_x or k_y that satisfy the relation $k_x^2 + k_y^2 < (nk_0)^2$, meaning that the evanescent waves are converted back into propagating waves.[23] So this convolution mechanism may also exist in Cr nanoholes to convert the evanescent waves into propagating waves. It should be noted that the depth of the Cr nanoholes in Fig. 2 is smaller than the wavelength, which may result in only a small portion of the evanescent wave being converted into a propagating wave through convolution with the exit aperture of the Cr nanoholes. This is further supported by the weaker light intensity above the Cr nanohole in Fig. 4(c). Figure 4(d) also shows that the evanescent waves around the PS nanospheres are radiated into the far field. Unlike the case of Cr nanoholes, the PS nanospheres change the total reflection condition for the generation of evanescent waves on the waveguide surface and convert them into propagating waves by coupling.

The LTms surface without sample placement shows a uniform dark field when observed through an optical microscope. The reason is that the evanescent waves on the surface of the LTms are uniformly distributed and confined within a range of 200 nm, while the objective lens does not capture any radiated light emitted from the surface of the LTms. However, when a sample is placed on the LTms surface, it disrupts the distribution of the evanescent wave and scatters the light into the far field. As a result, changes in the intensity of the scattered light collected by the objective lens correspond to structural information about the sample on the LTms.

In addition, ESM-LTms is also affected by spatial frequency shift (SFS) in evanescent light illumination. The scattered light of a sample $o(r)$ illuminated by a evanescent light with a wave vector k_e can be written as $s(r) = o(r)e^{ik_e r}$, where $r = (x, y)$ refers to the coordinates in the spatial domain. The detected intensity image of the sample is

07 August 2024 01:21:30

Published under an exclusive license by AIP Publishing

given by equation $I(r) = |F^{-1}(O(k - k_e) \times H(k))|^2$, where $O(k)$ is the Fourier spectrum of the $o(r)$, $H(k)$ is the optical transfer function (OTF) of the imaging system, and $k = (k_x, k_y)$ is the coordinate in the spatial frequency domain.[24] The spatial frequencies of the samples are thus shifted to new frequencies $k' = k - k_e$ under evanescent light illumination, which makes it possible to transfer high spatial frequencies to the passband of a conventional optical imaging system. Consequently, high spatial frequencies along the propagation direction of evanescent light can be captured by a conventional optical imaging system, resulting in an improved resolution in that direction. Imaging resolution is determined by both the maximal aperture of the system, k_c, and the transverse wave vector that is provided by the evanescent light illumination, k_e, as $d_{xy} = \frac{2\pi}{k_c + k_e}$, where k_c is equal to NAk_0 for label-free imaging.[25,26] Therefore, the theoretical resolution limit with label-free evanescent light illumination can be formulated as $d_{xy} = \frac{\lambda}{NA+a}$, where a is equal to $\frac{k_e}{k_0}$.

Subsequently, we investigated the imaging resolution of ESM-LTms for weakly scattering samples by simulating waveguide-based ESM for imaging PS nanospheres arranged in squares. The scattered waves from the PS nanospheres are first collected by a monitor and then decomposed into plane waves with different propagation angles. The low-pass filtering characteristic of the objective lens with an NA of 0.9 is emulated by selectively eliminating plane waves at angles greater than 65° and finally focusing the light that passes through to the image plane. The results presented in Fig. 5(a) demonstrate that the resolution of the evanescent light illumination imaging is influenced by the propagation direction of the evanescent wave. Specifically, when the transverse wave vector of the evanescent wave on the surface of the waveguide is $2\,k_0$, it can resolve a minimum edge-to-edge distance of 250 nm in the x-direction, while only 600 nm can be resolved in the y-direction. The resolution increases as the transverse wave vector of the evanescent wave increases, as shown in Fig. 5(b). When the transverse wave vector of the evanescent wave is $4\,k_0$, the simulated ESM-LTms can resolve a minimum edge-to-edge distance of 200 nm in the x-direction, while also improving resolution in the y-direction. The imaging results of a simulated conventional optical microscopy are shown in Fig. 5(c), demonstrating equal resolution in both x- and y-directions. In addition, it is capable of resolving the minimum edge-to-edge distance of 500 nm. Figure 5 reveals the superior resolution of evanescent light illumination microscopy compared to conventional optical microscopy for imaging weakly scattering objects. It also shows that the imaging resolution of evanescent light illumination is affected by its transverse wave vector and exhibits directional variability. In addition, the resolution along the propagation direction of the evanescent wave is improved but deviates from the theoretical value ($\frac{2\pi}{k_c + k_e}$). The reason is that the theoretical value requires the imaging system to detect all spatial frequencies of the sample within an OTF with a radius of $k_c + k_e$, and it is not possible to achieve a perfect two-dimensional OTF using evanescent wave illumination in a single incidence direction.

The utilization of waveguide-based ESM represents an efficacious approach for enhancing conventional optical microscopy. Evanescent waves exhibit a localized near-field characteristic and propagate orthogonally to the imaging optical path, thereby minimizing background noise and isolating valuable scattered signals. Because the ESM-LTms does not apply fluorescence super-resolution imaging methods[11,12] and image reconstruction algorithms,[24,26,27] its resolution is not comparable to other super-resolution imaging techniques. However, conventional label-free direct imaging methods offer unparalleled advantages, including real-time imaging, which maximizes the preservation of *in situ* information regarding the sample. The ESM-LTms offers a straightforward and dependable solution to meet these requirements. In addition, due to the localized near-field characteristic of evanescent light, ESM-LTms suffers from the same challenges as other waveguide-based evanescent light illumination imaging when imaging samples far away from the interface.

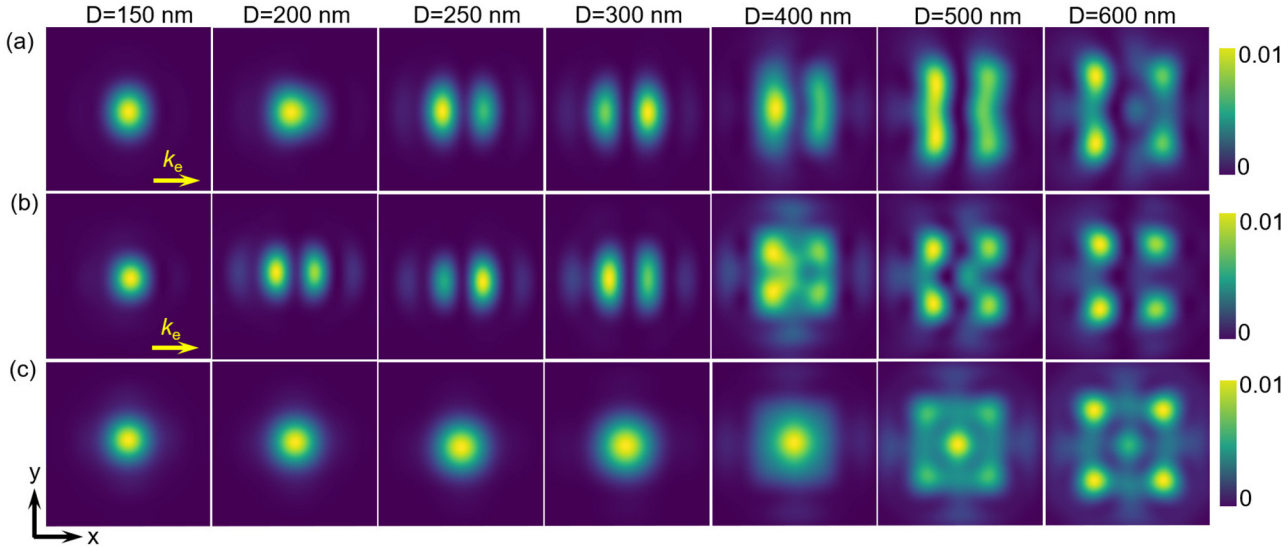


FIG. 5. Simulated ESM-LTms imaging of 100 nm diameter PS nanospheres arranged in squares. (a) and (b) The ESM-LTms images corresponding to evanescent waves with transverse wave vectors of $2\,k_0$ and $4\,k_0$, respectively. (c) The conventional diffraction-limited images. The edge-to-edge distances of adjacent PS nanospheres are 150, 200, 250, 300, 400, 500, and 600 nm, respectively.

07 August 2024 01:21:30

Published under an exclusive license by AIP Publishing

In summary, we present an approach for implementing a waveguide-based ESM using the LTms. The approach uses an LT waveguide that provides evanescent light illumination as a microscope slide to aid optical microscopy. We demonstrate that LTms can enable conventional optical microscopy with high imaging resolution and contrast. Compared to conventional waveguide-based ESM, LTms offers advantages such as not requiring complex nanofabrication to achieve high-contrast imaging with a large FOV efficiently and economically, while also being easier to integrate with conventional optical microscopes.

This work was financially supported by the National Natural Science Foundation of China (Grant No. 62375135) and the Scientific Research Starting Foundation of Nanjing Normal University (Grant No. 184080H201B122).

AUTHOR DECLARATIONS

Conflict of Interest

The authors have no conflicts to disclose.

Author Contributions

Songlin Yang: Conceptualization (equal); Investigation (lead); Methodology (equal); Software (equal); Supervision (equal); Writing – original draft (lead); Writing – review & editing (equal). **Qihao Sun:** Software (equal). **Yurong Cao:** Methodology (equal). **Yong-Hong Ye:** Funding acquisition (lead); Methodology (equal); Resources (equal); Writing – review & editing (equal). **Jiayu Zhang:** Conceptualization (equal); Resources (equal); Supervision (equal).

DATA AVAILABILITY

The data that support the findings of this study are available from the corresponding author upon reasonable request.

REFERENCES

[1]E. Betzig, G. H. Patterson, R. Sougrat, O. W. Lindwasser, S. Olenych, J. S. Bonifacino, M. W. Davidson, J. Lippincott-Schwartz, and H. F. Hess, "Imaging intracellular fluorescent proteins at nanometer resolution," Science **313**, 1642–1645 (2006).
[2]M. J. Rust, M. Bates, and X. Zhuang, "Sub-diffraction-limit imaging by stochastic optical reconstruction microscopy (STORM)," Nat. Methods **3**, 793–796 (2006).
[3]P. Zhang, G. Ma, W. Dong, Z. Wan, S. Wang, and N. Tao, "Plasmonic scattering imaging of single proteins and binding kinetics," Nat. Methods **17**, 1010–1017 (2020).
[4]X.-L. Zhou, Y. Yang, S. Wang, and X.-W. Liu, "Surface plasmon resonance microscopy: From single-molecule sensing to single-cell imaging," Angew. Chem., Int. Ed. **59**, 1776–1785 (2020).
[5]D. Axelrod, "Cell-substrate contacts illuminated by total internal reflection fluorescence," J. Cell Biol. **89**, 141–145 (1981).
[6]D. Li, L. Shao, B.-C. Chen, X. Zhang, M. Zhang, B. Moses, D. E. Milkie, J. R. Beach, J. A. Hammer, M. Pasham, T. Kirchhausen, M. A. Baird, M. W. Davidson, P. Xu, and E. Betzig, "Extended-resolution structured illumination imaging of endocytic and cytoskeletal dynamics," Science **349**, aab3500 (2015).
[7]S. Foylan, W. B. Amos, J. Dempster, L. Kölln, C. G. Hansen, M. Shaw, and G. McConnell, "MesoTIRF: A prism-based Total Internal Reflection Fluorescence illuminator for high resolution, high contrast imaging of large cell populations," Appl. Phys. Lett. **122**, 113701 (2023).
[8]R. Diekmann, Ø. I. Helle, C. I. Øie, P. McCourt, T. R. Huser, M. Schüttpelz, and B. S. Ahluwalia, "Chip-based wide field-of-view nanoscopy," Nat. Photonics **11**, 322–328 (2017).
[9]A. Archetti, E. Glushkov, C. Sieben, A. Stroganov, A. Radenovic, and S. Manley, "Waveguide-paint offers an open platform for large field-of-view super-resolution imaging," Nat. Commun. **10**, 1267 (2019).
[10]A. K. Engdahl, S. Belle, T.-C. Wang, R. Hellmann, T. Huser, and M. Schüttpelz, "Large field-of-view super-resolution optical microscopy based on planar polymer waveguides," ACS Photonics **8**, 1944–1950 (2021).
[11]Ø. I. Helle, D. A. Coucheron, J.-C. Tinguely, C. I. Øie, and B. S. Ahluwalia, "Nanoscopy on-a-chip: Super-resolution imaging on the millimeter scale," Opt. Express **27**, 6700–6710 (2019).
[12]Ø. I. Helle, F. T. Dullo, M. Lahrberg, J.-C. Tinguely, O. G. Hellesø, and B. S. Ahluwalia, "Structured illumination microscopy using a photonic chip," Nat. Photonics **14**, 431–438 (2020).
[13]P. Zhang, L. Zhou, R. Wang, X. Zhou, J. Jiang, Z. Wan, and S. Wang, "Evanescent scattering imaging of single protein binding kinetics and DNA conformation changes," Nat. Commun. **13**, 2298 (2022).
[14]B. Agnarsson, A. Lundgren, A. Gunnarsson, M. Rabe, A. Kunze, M. Mapar, L. Simonsson, M. Bally, V. P. Zhdanov, and F. Höök, "Evanescent light-scattering microscopy for label-free interfacial imaging: From single sub-100 nm vesicles to live cells," ACS Nano **9**, 11849–11862 (2015).
[15]B. Agnarsson, H. K. Wayment-Steele, F. Höök, and A. Kunze, "Monitoring of single and double lipid membrane formation with high spatiotemporal resolution using evanescent light scattering microscopy," Nanoscale **8**, 19219–19223 (2016).
[16]B. Agnarsson, M. Mapar, M. Sjöberg, M. Alizadehheidari, and F. Höök, "Low-temperature fabrication and characterization of a symmetric hybrid organic–inorganic slab waveguide for evanescent light microscopy," Nano Futures **2**, 025007 (2018).
[17]N. Jayakumar, F. T. Dullo, V. Dubey, A. Ahmad, F. Ströhl, J. Cauzzo, E. M. Guerreiro, O. Snir, N. Skalko-Basnet, K. Agarwal, and B. S. Ahluwalia, "Multimoded high-index contrast optical waveguide for super-contrast high-resolution label-free microscopy," Nanophotonics **11**, 3421–3436 (2022).
[18]D. J. Hill, C. W. Pinion, J. D. Christesen, and J. F. Cahoon, "Waveguide scattering microscopy for dark-field imaging and spectroscopy of photonic nanostructures," ACS Photonics **1**, 725–731 (2014).
[19]S. Ramachandran, D. A. Cohen, A. P. Quist, and R. Lal, "High performance, led powered, waveguide based total internal reflection microscopy," Sci. Rep. **3**, 2133 (2013).
[20]L. Priest, J. S. Peters, and P. Kukura, "Scattering-based light microscopy: From metal nanoparticles to single proteins," Chem. Rev. **121**, 11937–11970 (2021).
[21]C. F. Bohren and D. R. Huffman, *Absorption and Scattering of Light by Small Particles* (John Wiley & Sons, Ltd., 1998).
[22]L. Novotny and B. Hecht, *Principles of Nano-Optics* (Cambridge University Press, 2006).
[23]Y. Ben-Aryeh, "Transmission enhancement by conversion of evanescent waves into propagating waves," Appl. Phys. B **91**, 157–165 (2008).
[24]C. Pang, J. Li, M. Tang, J. Wang, I. Mela, F. Ströhl, W. S. Lisa Hecker, X. L. Qiulan Liu, Y. Wang, H. Zhang, M. Xu, X. Zhang, X. Liu, Q. Yang, and C. F. Kaminski, "On-chip super-resolution imaging with fluorescent polymer films," Adv. Funct. Mater. **29**, 1900126 (2019).
[25]X. Hao, X. Liu, C. Kuang, Y. Li, Y. Ku, H. Zhang, H. Li, and L. Tong, "Far-field super-resolution imaging using near-field illumination by micro-fiber," Appl. Phys. Lett. **102**, 013104 (2013).
[26]M. Tang, Y. Han, D. Ye, Q. Zhang, C. Pang, X. Liu, W. Shen, Y. Ma, C. F. Kaminski, X. Liu, and Q. Yang, "High-refractive-index chip with periodically fine-tuning gratings for tunable virtual-wavevector spatial frequency shift universal super-resolution imaging," Adv. Sci. **9**, 2103835 (2022).
[27]M. Tang, X. Liu, Z. Wen, F. Lin, C. Meng, X. Liu, Y. Ma, and Q. Yang, "Far-field superresolution imaging via spatial frequency modulation," Laser Photonics Rev. **14**, 1900011 (2020).

07 August 2024 01:21:30

Published under an exclusive license by AIP Publishing